Electrical Excitation Waves in the Myocardium: The Equivalent Dispersion Dependence

O. ANOSOV, S. BERDYSHEV, I. KHASSANOV, B. HENSEL
Department of Biomedical Engineering, Friedrich-Alexander University Erlangen-Nuremberg, Erlangen, Germany

Summary

We used the formalism of wave-packet propagation in passive media to characterize the spread of electrical excitation in excitable media, namely the myocardium. We introduced equivalent concepts of group and phase velocities, attenuation coefficient, and refraction index to describe the myocardial excitation wave, and applied the wavelet approach to construct an analogue of the classical dispersion dependence for active media – the "equivalent dispersion dependence." Using wavelet decomposition, we developed a method for reconstructing the equivalent dispersion dependence for the myocardium on the basis of electrical intracardiac signals that are measured in two spatially separated points. We applied this novel method to two different sets of experimental data and to data obtained from a numerical simulation of the atrial myocardium. We have shown that the introduced equivalent dispersion dependence under physiologic conditions is similar to the one obtained for resonant wave-medium interaction. The analysis of both experimental data sets clearly shows that the number of cardiac cycles with a resonant form of the equivalent dispersion dependence predominates in the normal state of the myocardium while it decreases before the onset of atrial fibrillation. We hypothesized that an increasing number of non-resonant cardiac cycles is a precursor of atrial fibrillation and thus can serve to predict fibrillation at an early stage before its onset. The proposed concept can be applied to investigate the properties of the atrial and ventricular myocardium.

Key Words

Wave-packet propagation, equivalent dispersion dependence, wavelet analysis, active medium, passive medium

Introduction

The theory of excitable media has proven to be a valuable tool for the investigation of the myocardial substrate, especially for the propagation of electrical excitation [1-4]. Wave propagation in the myocardium is a so-called autowave process that is commonly observed in a large number of systems in nature called active media [2]. While waves in passive media generally only transfer energy to the medium, autowaves also receive energy from the active medium. The excitation waves are thus not simply coupled to the medium in which they propagate, but are generated by the medium itself. In other words, they are well-defined states of the medium. It should be noted that this fact imposes a severe restriction on the analysis of wave propagation, since it is not possible to study monochromatic waves in active media.

The shape of an excitation wave depends mainly on the local microscopic properties of the medium, and its analysis allows us to draw conclusions about the state of the myocardium and its pathologic alterations. This local view of the myocardium is expanded by simultaneously analyzing the signals from more than one electrode. An additional analysis may consist in determining the velocity of the spread of the electrical excitation, which is an important parameter in connection with atrial or ventricular fibrillation (AF or VF) and other cardiac problems. In this article, we expand this approach by determining the velocity not only for the wave as a whole, but for its spectral components, more precisely for its wavelet components. The developed method is highly sensitive to inhomogeneities in the microscopic properties of the medium. These inhomo-

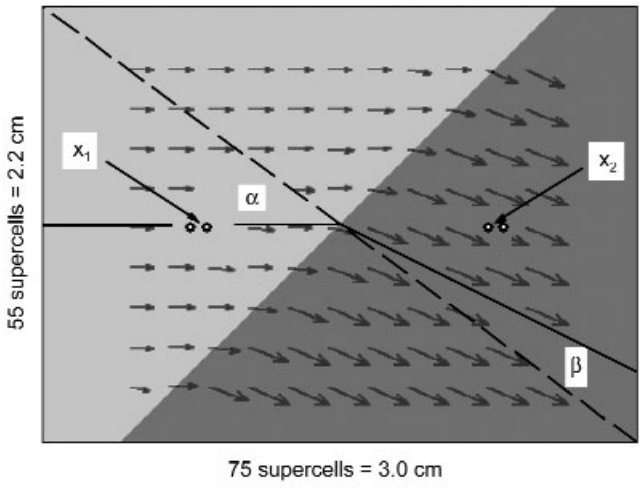

Figure 1. Setup for the numerical simulation of the wave propagation in human atrial myocardium using Nygren's description of ion channel dynamics [5]. The model consists of a slab of 75 x 75 x 4 cubic supercells, each with an edge length of 400 μm. The coupling of the supercells to the left and right of the 45° border has been adjusted so that the ratio of the velocities of propagation of the electrical excitation to the left and to the right is v_l/v_r = 1.75. The equivalent index of refraction is obtained from the angles α = 45° and β = 23° by n = sin α / sin β = 1.81.

geneities, in turn, are widely considered to be of great importance for the development of AF or VF.

Despite the different nature of passive and active media, the fundamental mechanisms of wave propagation remain the same. In both cases, the dispersion results from an interaction between the wave and the medium. The interaction depends on the frequency of the wave or its spectral components, be it a passive or active medium. Consequently, refraction is also observed in active media (see example in Figure 1 [5]), and the index of refraction obeys the same physical laws that are valid for passive media [6]. Thus we can reasonably assume that the dispersion law provides the theoretical framework for a quantitative treatment of wave propagation in active media.

Resonances of the interaction between the wave and the medium occur whenever their temporal or spatial characteristics match; in the present case, the time constants for the opening of ensembles of ion channels in the membrane or the characteristic length scales of inhomogeneities in the myocardial properties. These resonances do not occur because of a match with the heart rate, but are due to the microscopic excitation of the myocardium by only a spectral component of the wave. These components generally have frequencies well above the heart rate (> 10 Hz).

In this paper, we propose using the formalism of wave dispersion theory [7] to evaluate the properties of the myocardium. Using wavelet decomposition, we developed a method for the reconstruction of an analogue of the dispersion dependence for the myocardium ("equivalent dispersion dependence") on the basis of electrical intracardiac signals that are measured in two spatially separated points of the myocardium. We have shown that the equivalent dispersion dependences (EDD) for the myocardium can have a form similar to the ones that are typically obtained in the case of resonant wave-medium interaction in passive media. We found that the number of cardiac cycles with a resonant form of the dispersion predominates in the normal state of the myocardium while it decreases early on, before the onset of AF. We hypothesized that an increasing number of non-resonant cardiac cycles is a precursor of AF, and thus can serve to predict fibrillation early on before its onset.

We note, however, that the interpretation of the resulting EDD must be performed with great care and should be limited to the fundamental features outlined above. The proposed approach is a linear approximation of nonlinear processes in the myocardium. The experimental results, however, show that this approximation can supply important information about the properties of the myocardium, at least in the non-chaotic regimen.

Dispersion Dependence and its Reconstruction

Wave-Packet Propagation in Dispersive Media

Macroscopic dispersion characteristics of a medium can be described by dispersion dependence – the frequency-dependent complex refraction index $\eta(f) = n(f) + i\delta(f)$. Here $n(f)$ is the real part of the refraction index of the medium. The imaginary part $\delta(f)$ characterizes the transmission of energy between the wave and the medium [7]. To start with, for simplicity let us consider a one-dimensional wave-packet propagating along the spatial coordinate x with time t. The wave can be represented by $w(x,t) = a(x,t)\cos\varphi(x,t)$, where $a(x,t)$ is the slowly varying envelope of the wave-packet. Let the signal have some mean frequency f_0, and the envelope have a distinct maximum. Then we can estimate the wave-packet group velocity v_g by the propagation velocity of the maximum of the envelope, and the phase velocity v_p by the propagation velocity of the constant phase $\varphi(x,t) = \varphi_0 = const$.

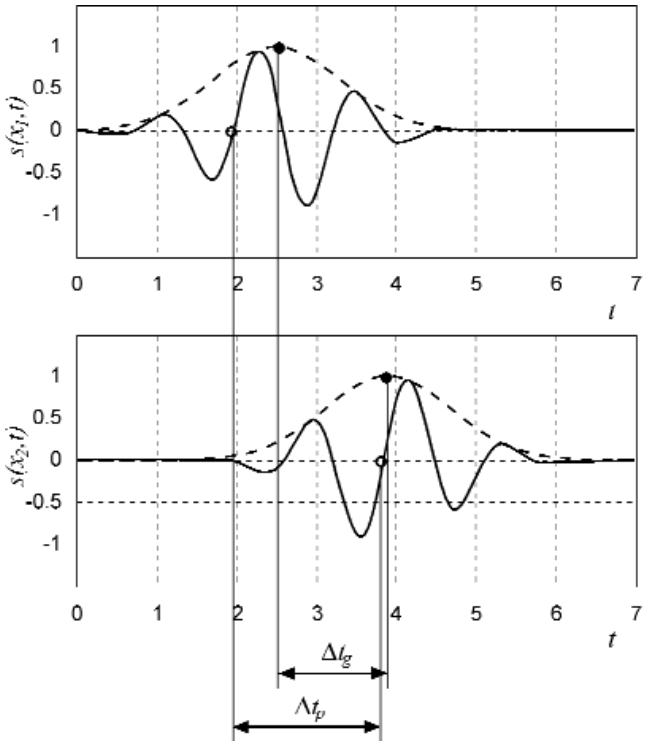

Figure 2. Estimate of the group v_g and the phase v_p velocities of the wave-packet propagation in the medium. Here, $s(x_1,t)$ and $s(x_2,t)$ are the time (t) dependent signals measured at points x_1 and x_2 separated by the distance r, Δt_g is the interval between the times when the envelope maximum passes the two points, and Δt_p is the time interval for the constant zero phase passing the same points. The group v_g and the phase v_p velocities are estimated as $v_g = r/\Delta t_g$ and $v_p = r/\Delta t_p$, respectively.

Assume that we have measured the signals $s(x_1,t)$ and $s(x_2,t)$, caused by propagation of the wave-packet $w(x,t)$ in two points, x_1 and x_2 that are separated by the distance r. Then, calculating the time interval Δt_g between the times when the envelope maximum passes the two points, we obtain an estimate for the group velocity $v_g = r/\Delta t_g$ over the distance r. Analogously, we can measure the time interval Δt_p for a constant phase, e.g., $\varphi_0 = 0$, and get the estimate of the phase velocity $v_p = r/\Delta t_p$ (Figure 2). The refraction index $n(f_0)$ of such a wave-packet can be calculated as the ratio of its group velocity v_g and its phase velocity v_p.

$$n(f_0) = \frac{v_g}{v_p} = \frac{\Delta t_p}{\Delta t_g}$$

For a wide class of signals $s(t)$ the envelope $a(t)$ and the phase $\varphi(t)$ can be calculated via the analytical signal $z(t) = s(t) + i\hat{s}(t)$, where $\hat{s}(t)$ is the Hilbert conjugate of $s(t)$ [8]. The envelope is then given by

$$a(t) = \sqrt{s^2(t) + \hat{s}^2(t)}$$

and the phase by

$$\varphi(t) = \operatorname{atan}\left(\hat{s}(t)/s(t)\right)$$

Thanks to the finiteness of the wave-packets, the imaginary part of the complex refraction index, the transmission coefficient $\delta(f_0)$, can be estimated as the ratio of the powers $E1$ and $E2$ of the signals measured at the two points:

$$\delta(f_0) = \frac{E_2}{E_1} = \frac{\int s^2(x_2,t)dt}{\int s^2(x_1,t)dt}$$

Although the dispersion properties of a passive medium, i.e., $n(f)$and $\delta(f)$ can best be studied by investigating their response to monochromatic excitations of different frequencies, this is not possible for the myocardium. In the course of one normal cardiac cycle, the excitation wave propagates as a single pulse. In this case, we can reconstruct the dispersion properties of the myocardium by applying the above-described dispersion approach to the wavelet components of the intracardiac signals decomposed in frequency space. We do not reconstruct the dispersion dependence in the full classical sense of a passive medium. In the case of the myocardium, we only define an equivalent, namely the EDD.

Wavelet Decomposition and the Wave-packet

Wavelet analysis is a mathematical tool that is widely applied to solve many problems in biology and medicine [9,10]. A wavelet set is a set of smooth and quickly vanishing oscillating functions with good localization both in frequency and time. Its components can be interpreted as single signals of short times with oscillating structures. Using wavelet analysis [11], a signal $s(t)$ can be represented as a superposition of functions, generated by dilatations and shifts of a mother wavelet $\psi(t)$

$$s(t) \approx \sum_j \int_{-\infty}^{\infty} C_j(a_j,\tau)\Psi(a_j,t-\tau)\,d\tau \qquad (1)$$

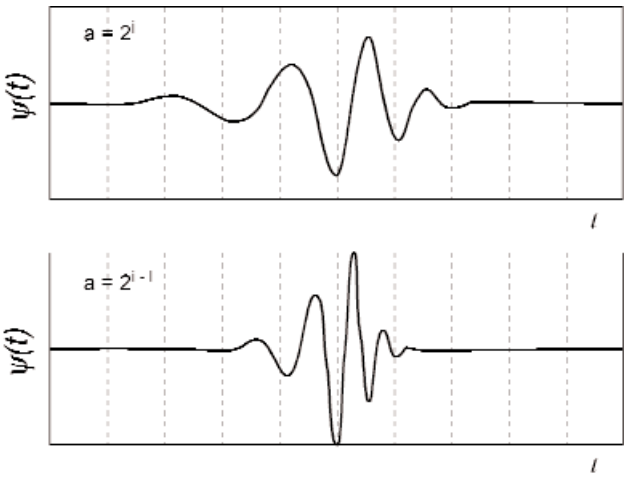

Figure 3. Daubechies wavelets $\psi(t)$ of the 7th order for two adjacent levels.

The parameter τ determines the shift of the wavelet $\psi(t)$ along the axis t, and the parameter a_j is the parameter of dilatation (the wavelet level). The coefficients C_j are by definition:

$$C_j(a_j,\tau) = \frac{1}{\sqrt{a}} \int_{-\infty}^{\infty} s(t)\,\Psi\left(\frac{t-\tau}{a_j}\right) dt \qquad (2)$$

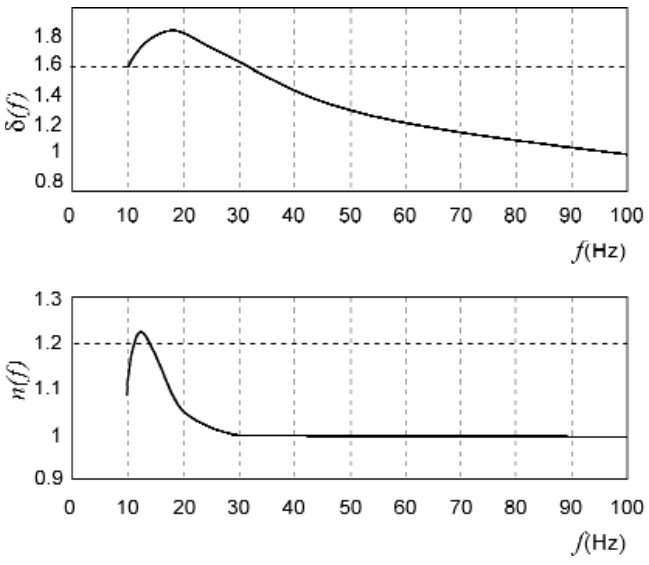

Figure 4. Frequency (f) dependence of the transmission coefficient $\delta(f)$ for the wavelet components (7th order Daubechies wavelet) of the bipolar signals $s(x_1,t)$ and $s(x_2,t)$ obtained in the numerical simulation of Figure 1.

where $a_j = 2^j$, $j = 0,1,2,\ldots$. The wavelet decomposition has features that are very important to the problem we are considering. Firstly, like the Fourier basis, the wavelet basis is orthogonal and allows the independent analysis of the individual signal components. Secondly, wavelets can be chosen to be quickly damping oscillating functions (see Figure 3), similar to the wave-packets under consideration. The transition from one wavelet level to the next is equivalent to a twofold compression of the time scale, or a twofold increase of the mean frequency ω_0. Thus, the wavelet basis is a set of wave-packets with an exponential frequency spacing of its components.

Let us consider some characteristic features of wavelet decomposition. According to Equation 1, the wavelet transformation allows us to substitute the initial signal $s(t)$ by the sum of component signals $s_i(a_i,t)$:

$$s(t) \approx \sum_j \left(\int_{-\infty}^{\infty} C_j(a_j,\tau)\,\Psi(a_j,t-\tau)\,d\tau \right) = \sum_j s_j(a_j,t) \qquad (3)$$

We will call them the "wavelet components" of the signal. In accordance with equation 3, each wavelet component is a convolution of an a_j-level decomposition coefficient $C_j(a_j,t)$ of the original signal $s(t)$ and the a_i-level wavelet $\psi(t)$ itself. Due to the finiteness of the wave-packet signal s, it follows from Equations 2 and 3 that the wavelet components s_j of each level a_j will be finite, i.e., will be a signal caused by wave-packets. Thus, the measured signal $s = s(t)$ caused by the propagation of the exitation wave can be interpreted as a sum of signals $s_j = s_j(t)$ caused by the simultaneous propagation of a set of wave-packets with different frequencies.

We apply the above introduced dispersion formalism not directly to the signals $s_1(t) = s_1(x_1,t)$ and $s_2(t) = s_2(x_2,t)$ measured at the points x_1 and x_2, but to their wavelet components $s_1(a_i,t)$ and $s_2(a_i,t)$ of the same level a_i. By calculating η for wavelet components of different levels, we finally obtain the complex refraction index and its dependence on the wavelet level $\eta(a) = n(a) + i\delta(a)$. Changing from the wavelet level a to the characteristic frequency f we get an estimate of the EDD frequency-dependent refraction index for excitation wave propagation in the myocardium, i.e., $\eta(f) = n(f) + i\delta(f)$.

For discrete signals, the frequency range available for analysis is restricted: the maximum frequency is

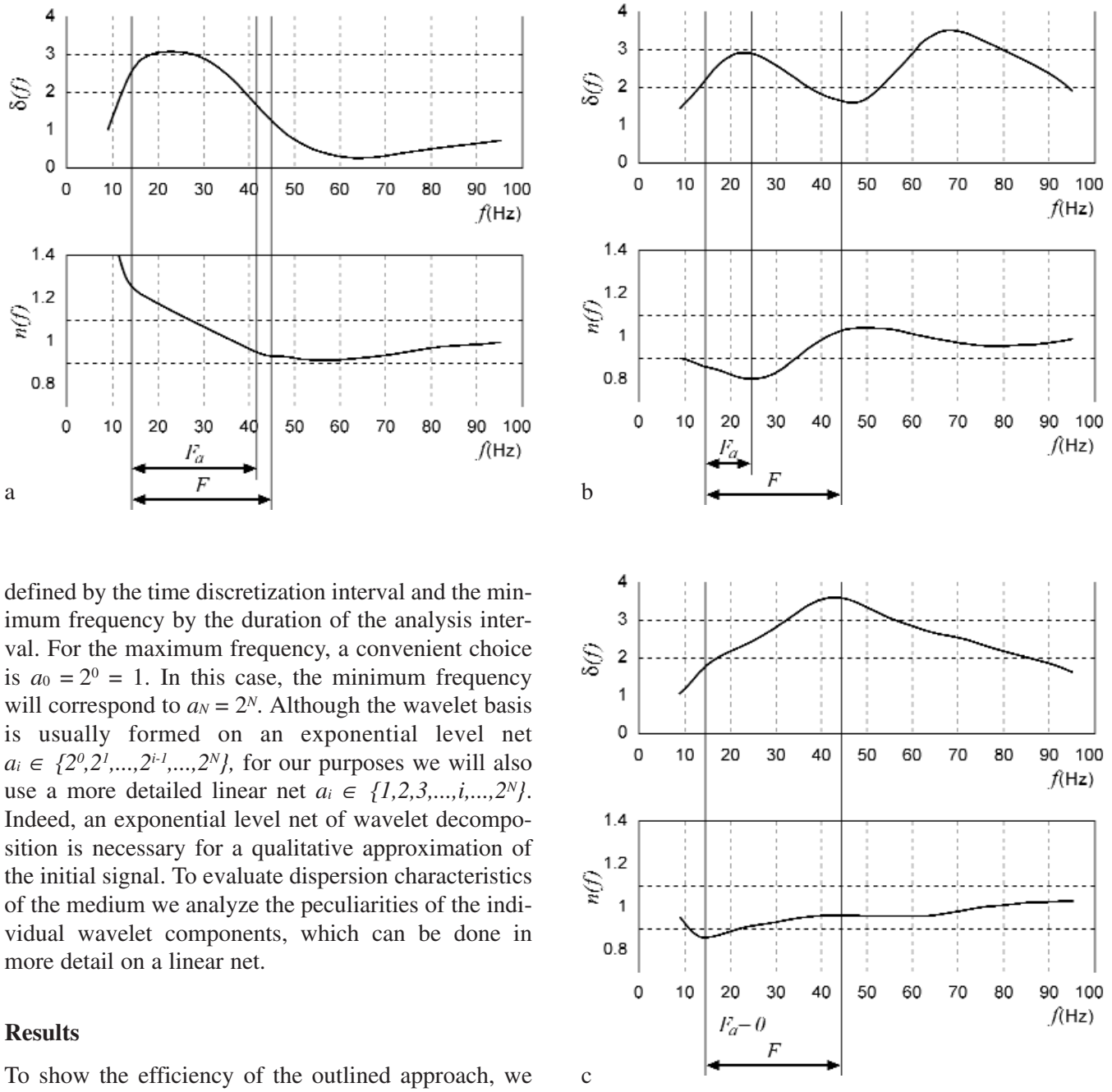

defined by the time discretization interval and the minimum frequency by the duration of the analysis interval. For the maximum frequency, a convenient choice is $a_0 = 2^0 = 1$. In this case, the minimum frequency will correspond to $a_N = 2^N$. Although the wavelet basis is usually formed on an exponential level net $a_i \in \{2^0,2^1,...,2^{i-1},...,2^N\}$, for our purposes we will also use a more detailed linear net $a_i \in \{1,2,3,...,i,...,2^N\}$. Indeed, an exponential level net of wavelet decomposition is necessary for a qualitative approximation of the initial signal. To evaluate dispersion characteristics of the medium we analyze the peculiarities of the individual wavelet components, which can be done in more detail on a linear net.

Results

To show the efficiency of the outlined approach, we applied it to data obtained from a numerical simulation of the human atrial myocardium and to two different sets of experimental data. We demonstrated the capability of the method to characterize the state of the atrial myocardium with the objective of revealing precursors for the occurrence of AF.

Reconstruction of EDD for a Wave Refraction on the Inclined Border

Wave "optics" in active media have already been numerically studied for reaction-diffusion systems

Figure 5. Three examples of the frequency (f) dependence of the transmission coefficient δ and of the refraction index n evaluated for the IEGM wavelet components. Measurements in patient C (panel c) were stopped due to atrial fibrillation paroxysms. No rhythm disturbances were revealed in patients A (panel a) and B (panel b). The analysis was performed on the basis of the 7th level Daubechies wavelet. Here, F is the band of analyzed frequencies and F_a is the band of anomalous dispersion (dn/df < 0). Patient C demonstrated no anomalous dispersion in the band of analysed frequencies.

using the Brusselator model [6]. In our studies, we performed simulations of the electrical wave propagation in human atrial myocardium using Nygren's description of ion channel dynamics [5]. The setup consists of a rectangular slab of 75 x 75 x 4 supercells representing the atrial myocardium. Each supercell has an edge length of 400 μm and is individually described by Nygren's formalism for atrial cells. The slab is embedded in a passive conductive medium representing surrounding tissue and blood. The supercells are mutually coupled by passive gap-junctions and additionally to the cleft space, i.e., the extracellular space between the cells. The resulting electrical circuit thus consists of two nested 3D resistor networks.

For the simulation, the differential equations that govern cell membrane dynamics are solved in each time increment, and subsequently the resulting current and voltage distribution is calculated. A wave propagating in the "virtual myocardium" can be triggered by stimulation with a voltage pulse at the "virtual electrodes." The microscopic properties of the supercells and the gap-junctions can be individually adjusted. In this way, the 45° "prism" of Figure 1 has been constructed. By varying the gap-junction conductivity to the left and the right of the interface the different velocities of wave propagation have been set, the ratio being $v_l/v_r = 1.75$. From the vector field in Figure 1, the refraction of the wave is evident, and a refraction index of the myocardium of $n = 1.81$ is obtained.

Applying our novel method of analysis to the electrical signals obtained from the two bipolar electrodes placed on the myocardium model (x_1 and x_2 in Figure 1), we obtain the expected equivalent resonance feature (Figure 4) that can also be reconstructed for experimental bipolar intracardiac electrograms (IEGM).

Dispersion Properties of the Atrial Myocardium Obtained from the Analysis of Bipolar Intracardiac Electrograms

We analyzed IEGM fragments (with durations between 12 s to 16 s) that were simultaneously measured with two bipolar leads introduced into the right atrium and the coronary sinus of patients with a high risk for AF. The IEGMs were sampled at frequencies of 2 kHz and 2.6 kHz. In two patients, the measurements were stopped due to triggered AF paroxysms. The EDD of the myocardium was evaluated for each cardiac cycle (on average 15 cycles per patient) using the 7th level Daubechies wavelets on a "linear scale." The frequency

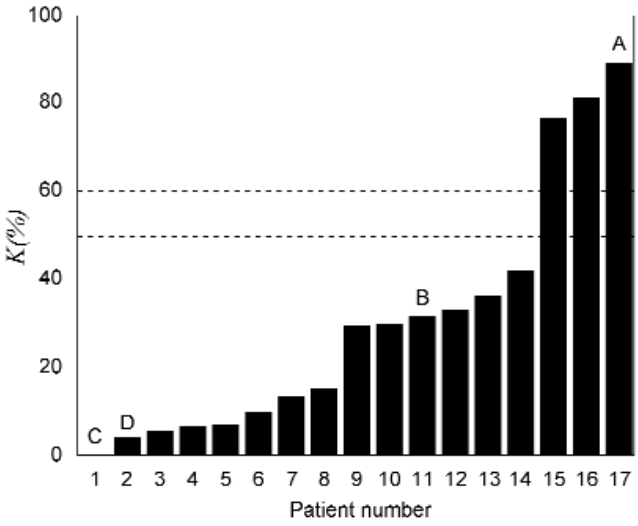

Figure 6. Mean values of the parameter K, characterizing the resonant coupling of the excitation wave and the myocardium in the right atrium, were evaluated for 17 patients. The measurement was interrupted in patients C and D due to atrial fibrillation paroxysms. Equivalent dispersion dependences typical for patients with normal sinus rhythm (patients A and B) and atrial fibrillation patients (patient C) are plotted in Figures 5a, 5b, and 5c, respectively.

band that could be analyzed ranged from 8.2 – 11.9 Hz to 68.2 – 29.6 Hz. The frequency limitations were due to the signal waveform, the cardiac cycle duration, and the noise level.

Figure 5 depicts three examples of the frequency dependence of the transmission coefficient δ and of the refraction index n evaluated for the IEGM wavelet components. As can be seen for patient A (Figure 5a, top), the transmission coefficient $\delta(f)$ has a peak with a maximum at 25 Hz. The refraction index $n(f)$ demonstrates anomalous dispersion ($dn/df < 0$) in the range of the peak (Figure 5a, bottom). For patient B, the transmission coefficient $\delta(f)$ also has a peak in the region of 25 Hz (Figure 5b, top), but the region of the refraction index is smaller than in the first case (Figure 5b, bottom). The transmission coefficient $\delta(f)$ for patient C also has a peak (Figure 5c, top), but it is less pronounced and shifted to higher frequencies with its maximum at about 45 Hz. The refraction index (Figure 5c, bottom) demonstrates a very small region of anomalous dispersion in this case. The peak in the transmission coefficient together with the anomalous dispersion depicted in Figure 5a is typical for a resonant

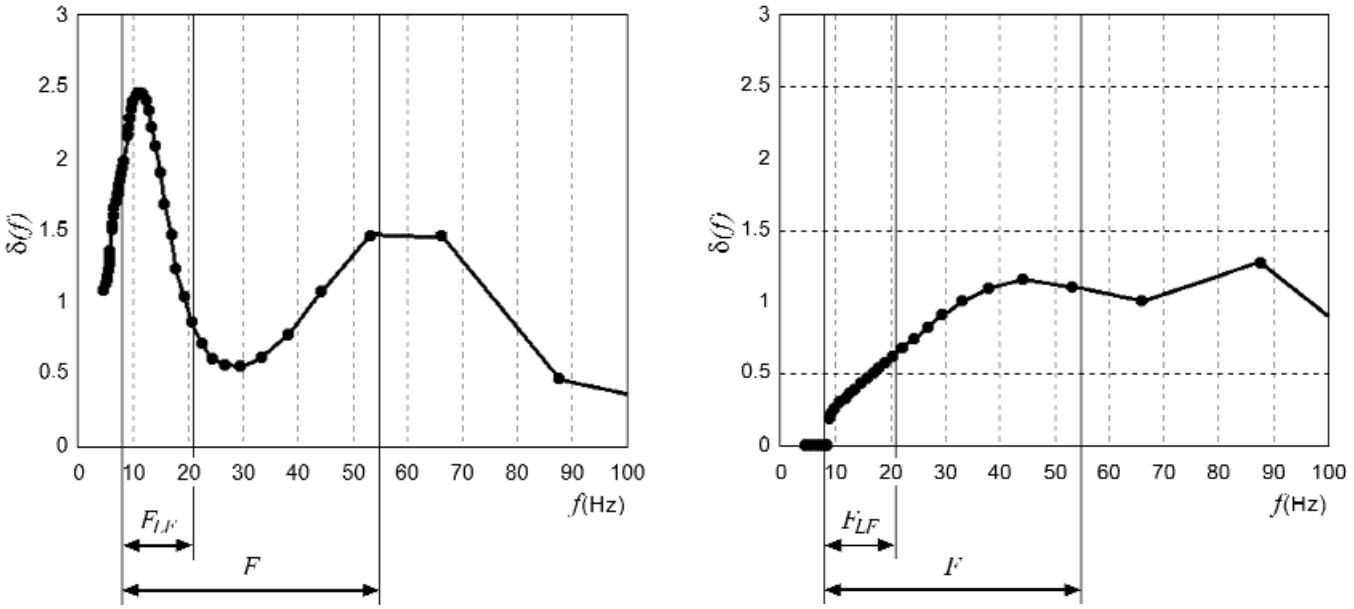

Figure 7. Frequency (f) dependence of the transmission coefficient δ for the wavelet components (7th order Daubechies wavelet) of the atrial monophasic action potential signals measured in the same patient, but in two different cardiac cycles. The resonance quality factor for the two beats (see text) has considerably different values: R = 44.9% (panel a) and R = 18.7% (panel b). Here again F is the band used for the analysis, and F_{LF} is the low frequency band.

wave-medium interaction. This observation reflects the resonant character of the interaction of the excitation wave with the myocardial cells. The resonance occurs in the range of 50 – 100 ms, values similar to those determined for cellular processes.

The excitation propagation in the atria of patient A demonstrates a pronounced resonant character of the coupling between the excitation wave and the myocardium. This observation should be expected in a physiologic or normal case; this concurs with the fact that patient A did not reveal any heart arrhythmia. Patient C, on the other hand, developed AF paroxysms in the course of the measurement, and consequently no resonant coupling features are observed. This decoupling of wave and medium can be interpreted as occurring due to a pathological state of the myocardium and might serve as a precursor for AF.

In order to quantify the state of the myocardium, we introduce a parameter for the resonance coupling properties of the myocardium as

$$K = 100\frac{F_a}{F}$$

(see Figure 5 for the frequency range definitions of F and F_a). The parameter K can range from 0 to 100%. The value K = 100% corresponds to F_a = 0, i.e., no anomalous dispersion in the analyzed frequency band, while K = 100% means that $F_a = F$, i.e., anomalous dispersion is observed over the whole frequency band. Figure 6 depicts the mean K values calculated for the IEGM records of 17 patients. The evaluation was performed for the frequency range F = 15 – 45 Hz with an averaging over 15 cardiac cycles. Patients A, B, and C (above) correspond to the letters A, B, and C in Figure 6. Patients C and D were the only ones to develop AF paroxysms during the measurement; they have the lowest K values (0% and 5%) among all patients included in the study.

The examples in this study demonstrate that EDD calculated for the wavelet components of the IEGM signals measured simultaneously at two distant sites in the atria has resonant characteristics in different non-AF patients, while it is absent or only just perceptible in AF patients. For patients with increasing risk of AF, one should expect a gradual smearing of the resonant peak and disappearance of the anomalous dispersion.

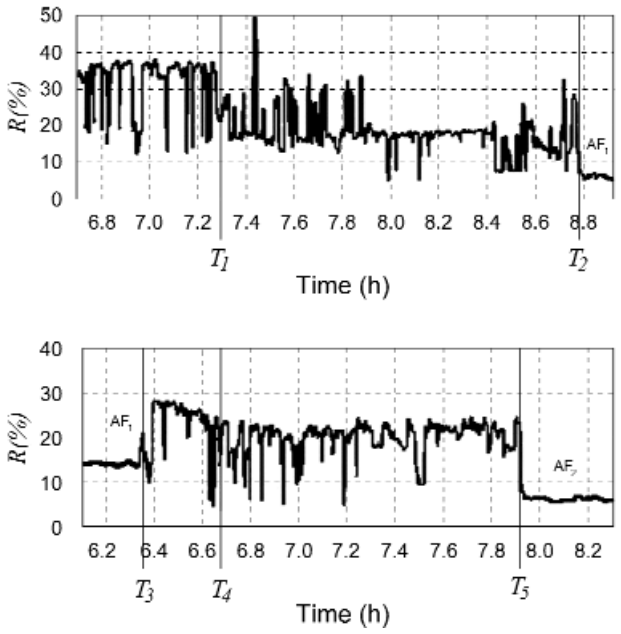

Figure 8. Dynamics of the resonance parameter R calculated from two monophasic action potentials. The monophasic action potentials (MAP) were recorded with two special MAP leads fixed on the atrial epicardium of the patient during the mitral valve replacement. Two sequential atrial fibrillation episodes (AF_1 and AF_2) were monitored. The bold line shows the mean value of R. T_2 and T_3 are the onset and the end of the AF_1 epsiode, T_5 is the onset of the AF_2 episode; T_1 and the transition from T_3 to T_4 mark significant changes of the mean value of R.

Dispersion Properties of the Atrial Myocardium in Patients Following Mitral Valve Replacement by Analysis of the Monophasic Action Potential

Mitral valve prosthesis patients are highly inclined to develop AF during the first few days following the operation. Over a 2-week period, we monitored the monophasic action potentials (MAP) in a group of patients immediately following valve replacement [12]. The MAPs were recorded at a sampling rate of 500 Hz using two special MAP leads positioned epicardially on the atria. We studied two AF episodes and analyzed long-term MAP records over several hours preceding the onset of AF. The dispersion and the time course of the resonance peak were studied on a beat-to-beat basis over more than 10000 excitations of the atrial myocardium. As in the analysis of IEGM fragments described before, the 7th order Daubechies wavelet was applied to the calculations. As the sampling frequency was rather low and the interlead distance too small, the $n(f)$ calculations were not satisfactory for the analysis. Thus, the analyses were carried out using the transmission coefficient $\delta = \delta(f)$. The dispersion characteristics of the transmission coefficient varied over time for each patient. For some beats, the δ had a very pronounced resonant character; for others no resonance features were evident. Figure 5 depicts two examples of the transmission coefficient $\delta(f)$ calculated for different cycles in the same patient. In Figure 7a distinct resonance peaks are present, while almost no resonance features are distinguishable in Figure 7b.

Analysis of the MAPs show that in the normal state (i.e., early on before the onset of AF) the number of cycles with resonance features is much higher than the number of non-resonant ones. Shortly before the onset of AF the number of non-resonant cycles increases and even becomes dominant. The dynamics of this process for developing AF is analyzed in the following manner. We introduce a parameter R characterizing the quality of the resonance in the transmission coefficient $\delta(f)$ and follow its variation over time until AF develops. The parameter is calculated from the total area S under the $\delta(f)$ curve over the whole analysed frequency range F and the partial area S_{LF} in the low frequency range F_{LF} (Figure 7):

$$R = 100\frac{S_{LF}}{S}$$

The parameter value is small without resonance in the range FLF, but increases with a more and more pronounced resonance. An analysis range F of 8 – 55 Hz was chosen. The low frequency range FLF was defined between 8 – 21 Hz. Using these frequency ranges, one obtains R = 44.9% with a pronounced resonance (Figure 7a) and R = 18.7% without any resonance features (Figure 7b). Figure 8 depicts the course of the resonance parameter R monitored over two sequential AF episodes in one patient. The bold line shows the mean value of R averaged over a sliding window of 21 cardiac cycles. The first AF episode occurred on the third day after the mitral valve replacement, at 8:48 (point T_2 in Figure 8), and lasted almost 20 hours, until 6:21 the next day (point T_3 in Figure 8). The second AF episode started at 7:56 of the same day (point T_5 in Figure 8) and lasted more than 6 hours. As can be seen in Figure 8, the resonance parameter R varied over the monitoring intervals. Until 7:20, the mean value of R lies around 37%, a value that is typical for resonant dispersion behavior (Figure 7a). Approximately 90 min

before the onset of the first AF episode (point T_1 in Figure 8), the mean value suddenly dropped to 18%, a value typical for a non-resonant dispersion (Figure 7b). The value of R remained at this level over the entire time interval preceeding the onset of the first AF episode. At the end of the episode, the mean value increased to 30% but again dropped to about 22% after 20 min (point T_4 in Figure 8). It remained at that level over an interval of 75 min prior to the beginning of the second AF episode. Thus, both AF episodes were marked by a significant decrease in the resonance parameter R some time before AF onset. A smaller resonance parameter R indicated a weaker coupling of the excitation wave to the atrial myocardium. The example described above shows that this developed approach can be applied to monitor patients with a high risk of AF in the post-operative period, and that the dispersion characteristics of the wavelet components derived for the IEGM signals measured at two sites of atrial myocardium can serve as AF precursors.

Discussion

We have developed a novel method for determining atrial myocardial properties by analyzing the dispersion that occurs for the wave propagation of electrical excitation. In this situation, we measured the electrical signals from two distant electrodes in the atria. The signals were decomposed using wavelets in order to obtain the frequency-dependent equivalent complex refraction index.

The classical method for determining the dispersion properties of a passive medium is to investigate its response to monochromatic excitations of different frequencies. As already outlined in the Introduction, this is not possible for active media such as atrial myocardium. Nevertheless, in this case it is possible to determine the dispersion by analyzing the "propagation" of the individual spectral components (wavelets) of the excitation. Our experimental data showed that by using this method, the dispersion properties of the atrial myocardium can be analyzed in the frequency ranges between 5 Hz and 100 Hz.

Strong spectral components are expected to originate from the fast upstroke of the action potential that occurs at the leading edge of the atrial excitation wave. This upstroke is due to the triggered opening of an ensemble of ion channels in the cell membrane. The characteristic time constant for this process is in the range from 5 ms to 100 ms, and thus corresponds to frequencies of 200 Hz and 10 Hz, respectively, in the physiologic case. Experimental [13,14] and numerical simulations [15] have determined that the threshold for the effective stimulation of the atrial myocardium by alternating currents strongly depends on the frequency. The threshold for the excitation is lowest in the frequency band between 10 Hz and 100 Hz. This fact corroborates the notion that externally applied 'monochromatic waves' of such frequencies are in 'resonance' with the myocardium.

Pathologic alterations of the myocardial properties are manifested in changes of the expression of ion channels and their characteristic time constants. Generally, these changes do not effect the myocardium as a whole but occur only locally. The result is a highly inhomogeneous distribution of the microscopic properties of the medium, and the refraction of the excitation wave logically depends on changes in the temporal and spatial correlation of these inhomogeneities. We have shown that the dispersion has a pronounced resonant character in the normal state of the myocardium, while the resonance gradually vanishes early before the onset of AF. By counting the relative number of resonant cycles, we obtain a measure for the risk of upcoming AF paroxysms.

Conclusion

This developed approach provides a promising instrument for monitoring the state of the myocardium and for predicting pathologic processes at an early stage.

References

[1] Winfree AT. The Geometry of Biological Time. Berlin: Springer. 1980.

[2] Zykov VS. Simulation of Wave Processes in Excitable Media. Manchester: Manchester University Press. 1988.

[3] Panfilov AV, Holden AV. Computational Biology of the Heart. New York: John Wiley & Sons. 1997.

[4] Focus Issue: Mapping and control of complex cardiac arrhythmias. Chaos. 2002; 12: 732-981.

[5] Nygren A, Fiset C, Firek L, et al. Mathematical model of an adult human atrial cell. Circulation Research. 1998; 82: 63-81.

[6] Sainhas J, Dilao R. Wave optics in reaction-diffusion systems. Phys Rev Lett. 1998; 80: 5216-5219.

[7] Landau LD, Lifshits EM. Electrodynamics of Continuous Media. Oxford: Pergamon Press. 1960.

[8] Panter D. Modulation, Noise and Spectral Analysis. San Francisco: McGraw-Hill. 1965.

[9] Bowman C, Newell AC. Natural patterns and wavelets. Review of Modern Physics. 1998; 70: 289-301.

[10] Blanco S, Figliola A, Quian Quiroga R. Time-frequency analysis of electroencephalogram series – Part III: Wavelet packets and information cost function. Phys Rev E. 1998; 57: 932-940.

[11] Daubechies I. Ten Lectures on Wavelets. (Cbms-Nsf Regional Conference Series in Applied Mathematics, No. 61). Philadelphia: Society for Industrial and Applied Mathematics (SIAM). 1992.

[12] Pichlmaier AM, Lang V, Harringer W, et al. Prediction of the onset of atrial fibrillation after cardiac surgery using the monophasic action potential. Heart. 1998; 80: 467-472.

[13] Irnich W, Silny J, de Bakker JMT. Fibrillation threshold induced by alternating current and alternating voltage. Biomed Tech (Berlin). 1974; 19: 62-65.

[14] Irnich W. Fundamental law of electrostimulation. Biomed Tech (Berlin). 1989; 34: 158-167.

[15] Müssig D, Hensel B, Schaldach M. Numerische Simulation des Verhaltens atrialen Myokards unter dem Einfluß von elektrischen Wechselfeldern. Biomed Tech (Berlin). 2001; 46 (Suppl) : 198-199.

Contact
Dr. Oleg Anosov
Department of Biomedical Engeneering
Friedrich-Alexander University
Erlangen-Nuremberg
Turnstrasse 5
D-91054 Erlangen
Germany
Fax: +49 9131 2 71 96
E-mail: oleg.anosov@biomed.uni-erlangen.de